Available online at www.sciencedirect.com

SciVerse ScienceDirect

Ceramics International 39 (2013) 3691–3697

CERAMICS INTERNATIONAL

www.elsevier.com/locate/ceramint

Luminescent and structural properties of manganese-doped zinc aluminate spinel nanocrystals

Mu-Tsun Tsai[a,*], Yee-Shin Chang[b], Ing-Bang Huang[a], Bo-Yu Pan[a]

[a]Department of Materials Science and Engineering, National Formosa University, Huwei, Yunlin 632, Taiwan
[b]Department of Electronic Engineering, National Formosa University, Huwei, Yunlin 632, Taiwan

Received 29 September 2012; received in revised form 11 October 2012; accepted 12 October 2012
Available online 22 October 2012

Abstract

Manganese-doped zinc aluminate spinel ($ZnAl_2O_4$:Mn; Mn = 0–6.0 mol%) phosphor nanoparticles were prepared by the sol–gel process. The effects of thermal annealing and dopant concentration on the structure, microstructure and luminescence of the powder phosphors were investigated. The X-ray diffraction (XRD) and Fourier transform infrared (FT-IR) results confirmed that a single-phase spinel started to crystallize at around 600 °C for the investigated powders. On heating at 600–1200 °C, the powders had the average crystallite sizes of around 12–33 nm. The crystallite size and lattice constant increased as the doping level of Mn increased. FT-IR spectra exhibited only absorption bands of the AlO_6 octahedral groups, which suggested that the powder phosphors mainly crystallized in a normal spinel structure. Scanning electron microscopy (SEM) investigations showed the primary particle sizes were around 20–25 nm for the powders annealed at 1000 °C, and less than ca. 50 nm for those annealed at 1200 °C. Photoluminescence (PL) spectra under UV or visible light excitation exhibited a strong green emission band centered at 510 nm, corresponding to the typical $^4T_1(^4G)$—$^6A_1(^6S)$ transition of tetrahedral Mn^{2+} ions. The most intense PL emission was obtained by exciting at 458 nm. The PL intensity was significantly enhanced by the improved crystallinity and diminished OH^- groups. Optimum brightness occurred at a doping of 3.0 mol% Mn.

Keywords: A. Powders; A. Sol–gel processes; $ZnAl_2O_4$:Mn; Photoluminescence

1. Introduction

Over the past two decades, the luminescent properties of inorganic phosphors have been extensively studied for their potential applications in displays and lighting devices. With the development of highly efficient low-voltage luminescent materials, oxide phosphors have attracted more attention for their better thermal and chemical stability and environmental friendliness in comparison with sulfides [1,2]. For solid-state lighting, bi-chromatic white light-emitting diodes (LEDs), consisting of an InGaN-based blue LED die and a yellow phosphor (e.g., YAG:Ce^{3+} based materials) which can be excited by blue light, have commonly been used as replacements for conventional incandescent lighting [3]. This type of white LEDs often has low color rendering properties, due to the lack of red and green light. In recent years, multiphosphor-converted white LEDs have been considered as viable alternatives, because they promise high color rendering properties and tunable color temperatures by applying the appropriate green, red, and/or blue phosphors, under blue or near-UV/UV excitation [4,5]. Of these, most commercially available white LEDs are prepared by pre-coating phosphors onto blue diode chips, because the luminous efficiency of blue chip based white LEDs is higher than that of n-UV/UV type. In order to improve color rendering of the white LEDs, it is essential to develop new phosphors using blue LED chips [5]. However, the photoluminescence of most oxide phosphors generally depends on UV excitation, because they have poor absorption in the visible light region. Therefore, it is necessary to find suitable blue-light excitable green-emitting phosphors with excellent photoluminescence properties for white LED applications.

Zinc aluminate ($ZnAl_2O_4$), a member of the spinel family, has been widely used as catalysts and catalyst supports due to its properties such as the high thermal and

*Corresponding author. Tel.: +886 5 5320731; fax: +886 5 6361981.
E-mail address: mttsai@ms23.hinet.net (M.-T. Tsai).

0272-8842/$ - see front matter © 2012 Elsevier Ltd and Techna Group S.r.l. All rights reserved.
http://dx.doi.org/10.1016/j.ceramint.2012.10.201

chemical stability, high mechanical resistance, low acidity and hydrophobicity [6,7]. $ZnAl_2O_4$ is a wide bandgap semiconductor ($E_g = 3.8$ eV), and is transparent to light of wavelengths above 320 nm, which makes it suitable for UV optoelectronic devices, transparent conductors, and optical coating applications in aerospace technology [8]. Recently, $ZnAl_2O_4$ has also attracted interest as a phosphor host material for application in thin film electroluminescence displays, mechano-optical stress sensors, and stress imaging devices [9,10]. Stress-stimulated luminescence was obtained for Mn-doped $ZnAl_2O_4$ powder prepared by a conventional solid-state reaction [10].

The luminescent properties of powder phosphors are well known to be strongly dependent on particle size, crystal structure, and uniform distribution of activators in the host lattice [10–14]. The synthesis of nanoparticle phosphors with narrow size distribution and uniform particle morphology showed promising luminescent characteristics, especially for flat panel display devices, as this potentially allows for higher packing density, lower scattering of the evolved light, less binder content, and higher screen resolution [9,12]. Compared with the traditional method, the sol–gel route offers several advantages, such as good stoichiometric control, high homogeneity, the ability to produce nanostructured powders and thin films, as well as low temperature processing. In our recent work [15], we prepared $ZnAl_2O_4$:Mn^{2+} phosphor by a simple sol–gel method. The powder phosphor annealed at 1000 °C exhibited a prominent green emission band peaking at around 512 nm under excitation by a 458 nm blue-light. However, the effects of thermal annealing and dopant concentration have not been investigated in detail. The purpose of the present work was thus to investigate the influences of activator concentration and heat-treatment condition on the structural evolution and luminescent properties of these powders.

2. Experimental

2.1. Synthesis

Mn-doped zinc aluminate powders were prepared by a sol–gel process using zinc chloride ($ZnCl_2$), aluminum isopropoxide ($Al(O\text{–}iC_3H_7)_3$), and manganese chloride ($MnCl_2 \cdot 4\ H_2O$) as the starting materials. Stoichiometric amounts of zinc chloride and aluminum isopropoxide were first dissolved in methanol. The mixed solution was stirred and refluxed at room temperature for 2 h, and then the desired amount of manganese chloride and a small content of deionized water (2.0 M ratio to Zn) were added for doping and hydrolysis. The transparent sols thus obtained were then kept at ambient temperature until gelation. The powder samples were prepared by drying the transparent gels at 100 °C in an oven and then grinding them, subsequently annealing the xerogel powders at various temperatures from 500 to 1200 °C for 2 h with a heating rate of 10 °C min^{-1}. The contents of Mn^{2+} were varied with 0–6.0 mol% of the Zn^{2+} concentration to investigate the effects of doping on structure and luminescence.

2.2. Characterization

The crystalline phase of the processed samples was examined by powder X-ray diffraction (XRD; Rigaku D/MAX-III) with Ni-filtered CuKα radiation. Infrared spectra were recorded in the 400–4000 cm^{-1} frequency range by Fourier transform infrared spectrometry (FT-IR; Bomen Michelson MB100) with KBr pellets. The morphology of the powder was observed by field-emission scanning electron microscopy (FE-SEM; JEOL JSM-6700F). Photoluminescence excitation and emission spectra were recorded at room temperature by a fluorescence spectrophotometer (F-4500, Hitachi), with a 150 W xenon lamp as the excitation source.

3. Results and discussion

3.1. The phase formation

Typical XRD patterns of $ZnAl_2O_4$:Mn xerogel powders annealed at different temperatures are shown in Fig. 1. The dried powders remained amorphous up to 500 °C annealing, and some weak diffraction peaks appeared after heating at 600 °C. The peaks and intensity increased with the annealing temperature from 600 °C to 1200 °C. All the reflections can be well indexed to a cubic $ZnAl_2O_4$ structure (JCPDS: 82-1043). No impurity lines were observed, indicating that the obtained $ZnAl_2O_4$:Mn phosphor powders had a single-phase spinel structure. On annealing at 800–1200 °C, the undoped powders were white while the doped powders were flesh-colored, indicating that the manganese ions were in the divalent state [16]. Since the Zn^{2+} and Mn^{2+} ions have similar oxidation states and ionic radii, the Mn^{2+} ions are well

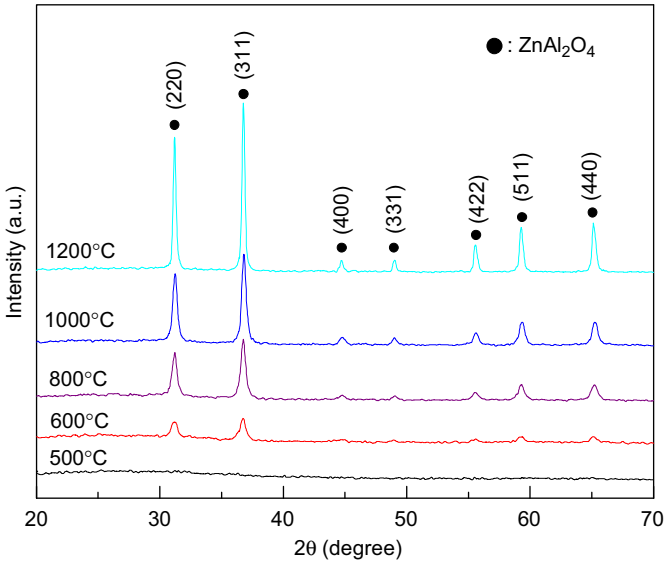

Fig. 1. XRD patterns of $ZnAl_2O_4$:3.0% Mn xerogel powders annealed at various temperatures.

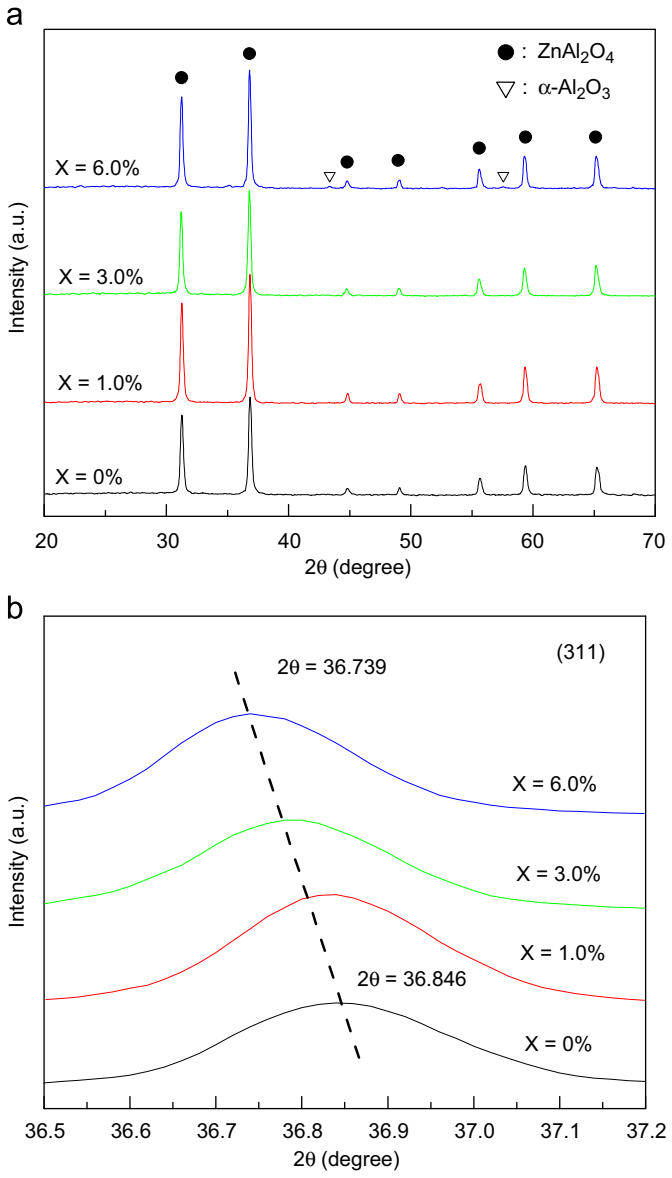

Fig. 2. (a) XRD patterns of $ZnAl_2O_4$:Mn^{2+} phosphors with various Mn concentrations (x) annealed at 1200 °C. (b) The peak positions of (311) diffraction plane as a function of Mn concentration.

dispersed as the substitutes of Zn^{2+} in the zinc aluminate host lattice after being heated. Consequently a homogeneous Mn^{2+}–$ZnAl_2O_4$ solid solution is expected, since no trace of impurity phase was detected. In addition, its crystallinity was improved as the annealing temperature increased. All of the undoped and Mn-doped samples had similar XRD features.

Fig. 2(a) shows the XRD patterns of $ZnAl_2O_4$:Mn^{2+} phosphors with various Mn concentrations (x) annealed at 1200 °C. The Mn^{2+} doping level did not cause significant change in the crystallinity of the samples. It is noted that all of the prepared powders annealed up to 1000 °C yielded no crystalline phases other than $ZnAl_2O_4$, regardless of the dopant concentration. With a further rise in temperature to 1200 °C, however, minor traces of α-Al_2O_3 were detected in those samples with a Mn content of 6.0 mol%. This can probably be attributed to the high doping content that could induce the occurrence of local chemical inhomogeneities at high temperature. Fig. 2(b) shows the (311) diffraction peaks shift toward a lower angle as the concentration of Mn increases. The shift in the peak position between the samples with a Mn doping level from $x=0\%$ to $x=6.0\%$ is $\Delta\theta=0.107^\circ$, indicating that the lattice constant slightly increased from 0.8086 to 0.8098 nm. This lattice expansion can be caused by the partial replacement of the smaller ionic radius of a tetrahedral Zn^{2+} ($r=0.06$ nm) by the larger four-coordinated Mn^{2+} ($r=0.066$ nm) [11]. In addition, if the Mn^{2+} substituted the octahedral Al^{3+} then this would also increase the lattice constant, because an octahedral Mn^{2+} ($r=0.083$ nm) is larger than the six-coordinated Al^{3+} ($r=0.0535$ nm).

The variation in crystallite size with the annealing temperature and doping concentration is shown in Fig. 3. The average crystallite size was estimated based on the broadening X-ray line of the reflections of (311) and (200) using Scherrer's equation. The mean crystallite sizes of the powder (Mn=3.0%) were found to vary from ~14 to 31 nm for samples annealed in the range of 600–1200 °C, and from ~29 to 33 nm for 1200 °C-heated samples with various Mn doping contents of 0–6.0%. On heating from between 600–1200 °C, the prepared powders had average crystallite sizes of around 12–33 nm, depending on the dopant content. In addition to the lattice constant, the XRD results also show that the crystallite size increased with an increase in the level of Mn doping. However, with appropriate doping content, the single-phase structure of the $ZnAl_2O_4$:Mn nanocrystal phosphors can certainly be synthesized by the sol–gel method presented in this study.

3.2. FT-IR absorption spectra

Fig. 4 shows FT-IR spectra of the $ZnAl_2O_4$:3.0% Mn^{2+} gel powders after thermal annealing at various temperatures.

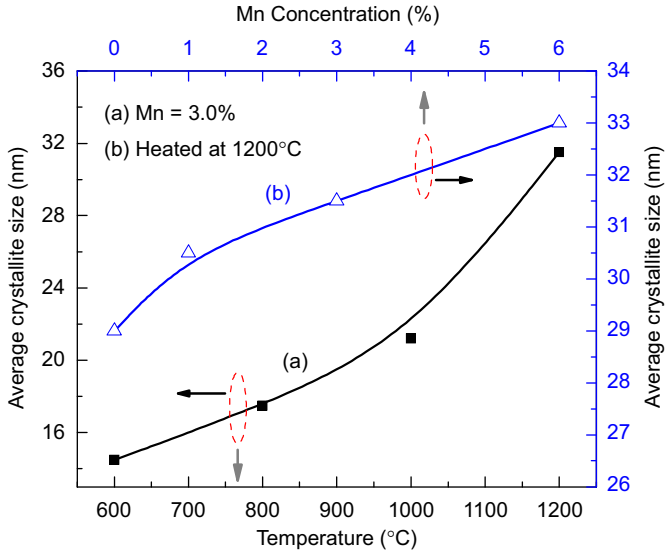

Fig. 3. Variation in crystallite size with the (a) annealing temperature and (b) Mn concentration for $ZnAl_2O_4$:Mn^{2+} phosphor powders.

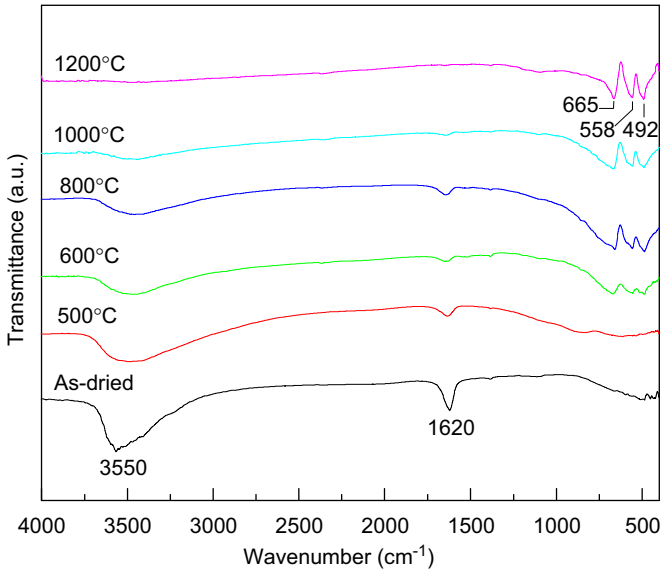

Fig. 4. Infrared spectra of $ZnAl_2O_4$:3.0% Mn^{2+} gel powders after thermal annealing at various temperatures.

The bands around 3550 $cm^{-1}$and 1620 cm^{-1} were assigned to the stretching mode of the OH^- group and adsorption due to water, respectively. These bands decreased in intensity as the annealing temperature rose and disappeared completely above 1000 °C. The powders annealed below 600 °C showed no evident absorption band other than the two ones mentioned above, which indicates the amorphous character of the samples. After heating to 600 °C and above, three well-defined bands characteristic of the $ZnAl_2O_4$ spinel structure were observed in range of 400–700 cm^{-1}. The bands at 665 and 558 cm^{-1} were related to the symmetric stretching (v_1) and symmetric bending (v_2) modes of AlO_6 groups, respectively [17], while the band at 492 cm^{-1} can be assigned to the asymmetric stretching (v_3) of AlO_6 [17]. These bands became sharper as the annealing temperature increased, which suggests the formation of more crystallized zinc aluminate. This result is in agreement with the findings from the XRD investigations.

Other samples also showed the similar FT-IR features. The octahedral coordination state of aluminum ions did not change significantly with Mn content. In addition, no peaks related to Al^{3+} in a tetrahedral coordination (e.g. AlO_4) were observed in the results. For spinel compounds, such as $MgAl_2O_4$, $CoAl_2O_4$, $ZnAl_2O_4$ and $SrAl_2O_4$, the octahedral groups (AlO_6) are expected to give the vibrational frequencies of v_1, v_2, and v_3 within the high-frequency region of 500–700 cm^{-1}, and undergo asymmetric bending (v_4) within the low-frequency region of 250–320 cm^{-1} [17–20]. If tetrahedral coordination (AlO_4) occurs (i.e., inversion occurs), the characteristic bands are expected to be within the range of 700–850 cm^{-1} and 250–320 cm^{-1}, respectively [17–19]. $ZnAl_2O_4$ usually presented two or three strong bands in the high-frequency region for the normal cubic spinel structure, moreover, the shape and position of the bands depended on the synthesis method [7,17]. In our case, the characteristic bands of AlO_6 are in good accordance with those in the literature, and the band related to AlO_4 was also absent from the IR spectra. These results are very similar to those of previous studies that examined pure and Mn-doped $ZnAl_2O_4$ normal spinel powders [7,20–24]. Accordingly, the IR investigations in this study show that the synthesized phosphor powders had a normal spinel characteristics, and thus it can be concluded that the prepared $ZnAl_2O_4$:Mn powders (Mn = 0–6.0 mol%) mainly crystallized in a normal spinel structure. The IR measurements are basically consistent with the XRD results, and confirm that $ZnAl_2O_4$ started to crystallize at around 600 °C, and that its crystallinity was enhanced as the annealing temperature increased.

3.3. Scanning electron microscopy

Fig. 5 shows SEM micrographs of the $ZnAl_2O_4$:3.0% Mn^{2+} phosphor powders annealed at 1000 °C and 1200 °C,

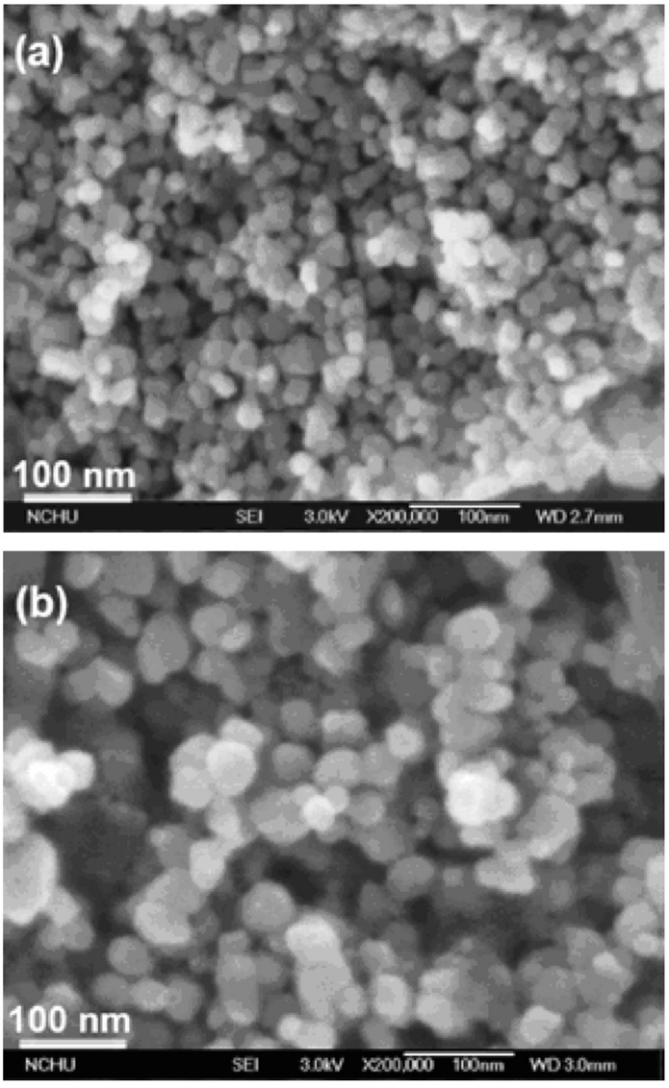

Fig. 5. SEM images of $ZnAl_2O_4$:3.0% Mn^{2+} phosphor powders annealed at (a) 1000 °C and (b) 1200 °C.

respectively. The phosphor powders consisted of granular structures with round morphology and soft agglomeration. The mean primary particle size was around 22 nm after calcining at 1000 °C, as measured from the scanning electron micrograph (Fig. 5a). This is close to the average crystallite size estimated from the XRD results, which suggests that each particle of the powders consisted of a single crystallite. The powder heated at 1200 °C had an increase in the size of the particles and degree of agglomeration, with a primary particle size of around 35–45 nm (Fig. 5b). The particle size and morphology of the phosphor powders did not show much variation among the investigated samples (Mn=0–6.0%), while the degree of agglomeration slightly increased as the dopant content or annealing temperature rose. Soft agglomeration is one of the characteristics of nanopowders. The powders examined in this work (Mn=0–6.0%) have primary particle sizes of around 20∼25 nm, with a narrow size-distribution for the 1000 °C-annealed samples, and less than ∼50 nm for the samples heated at 1200 °C for 2 h. Clearly, the sol–gel approach presented in this work has the capability of producing $ZnAl_2O_4$:Mn nanoparticle phosphors with a processing temperature ≤ 1200 °C.

3.4. PL spectra

Typical PLE and PL spectra of $ZnAl_2O_4:Mn^{2+}$ phosphors measured at room temperature are shown as a function of annealing temperature in Fig. 6. As shown in Fig. 6(a), the PLE spectra obtained by monitoring the green emissions at 510 nm exhibited four well defined bands at 360, 386, 427, and 458 nm, which can be assigned to the transitions of Mn^{2+} from the ground state $^6A_1$ (^6S) to $3d^5$ multiplets ^4E (^4D), $^4T2$ (^4D), ^4E $^4A_1$ (^4G), and $^4T_2$ (^4G), respectively [25]. Under the excitation of 458 nm, the PL spectra (Fig. 6b) revealed a single emission peak at around 510 nm corresponding to the typical $^4T_1(^4G)\rightarrow{}^6A_1(^6S)$ transition of Mn^{2+} ions. The luminescence of the Mn^{2+} ions is known to be affected by the host crystal field and site symmetry, which can vary the emission color from green to orange/red. Generally, Mn^{2+} emits green light when it located in a tetrahedral coordination (weak crystal field), and red light in an octahedral one (stronger crystal field) [11,12]. In our work, only the green emission at 510 nm is observed for all the investigated samples, suggesting that the Mn^{2+} ions mainly substituted at the tetrahedral Zn^{2+} sites in the host lattice. Similar results were also observed by Singh et al. [24], in which the $ZnAl_2O_4$:Mn powder was prepared using a combustion method. Consequently the green emissions are predominantly attributed to the d-d transition of tetrahedral Mn^{2+} ions.

As the temperature increased from 800 °C to 1200 °C, the peak intensities of the excitation and emission also increased. No emissions were detected in the 500 °C heated powder, as it remained amorphous. Compared with the powders annealed at 800 °C, the green emission was weak in the case of the sample annealed at 600 °C (see inset in Fig. 6b), due to its relatively poor crystallinity. The shape and peak position of the PL bands did not change with the increase in temperature, but the emission intensity increased significantly. Strongly enhanced luminescence was observed in the powder sample annealed at 1200 °C, and this is likely due to the increasing crystallinity of the host matrix and the elimination of residual OH^- groups. This agrees well with the XRD and FT-IR observations mentioned above, as shown in Figs. 1 and 4. In addition to the crystallinity, previous studies have demonstrated that decreasing the OH^- content can also enhance the emission intensity in phosphor materials [26,27]. The enhancement in luminescence properties seen in this work can thus be attributed both to the improvement in crystallinity, and to the decrease in residual hydroxyl groups or absorbed water, that occur with an increase in annealing temperature. The emission spectra also confirm that Mn^{2+} ions

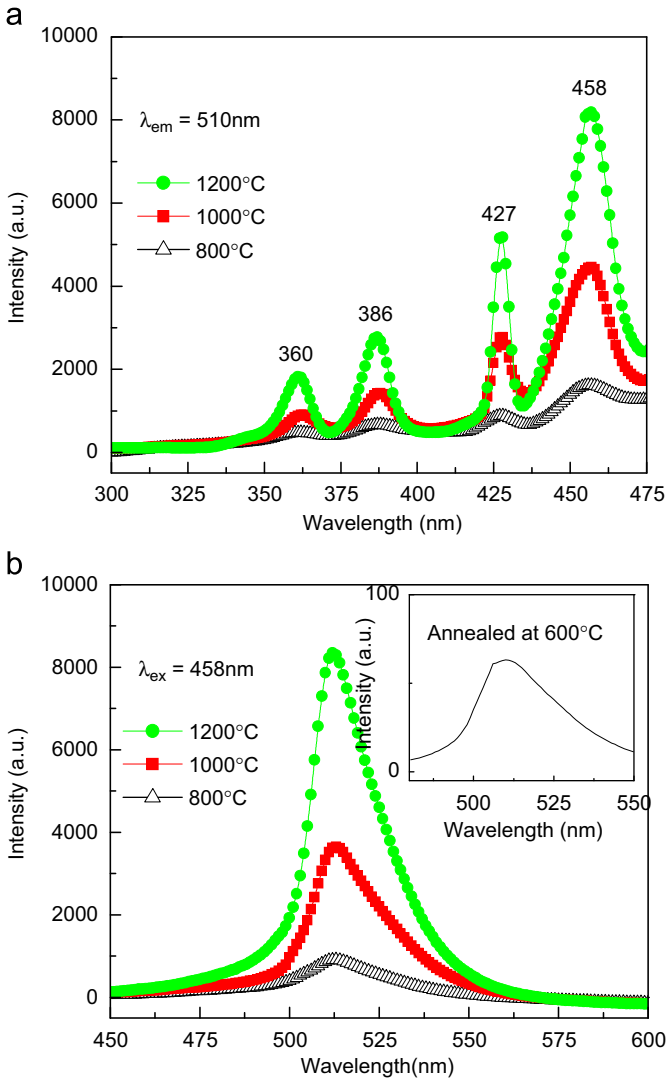

Fig. 6. PL (a) excitation and (b) emission spectra of $ZnAl_2O_4:Mn^{2+}$ powder phosphors after annealing in the temperature range of 800–1200 °C. The inset of (b) shows the emission spectra for the powder sample annealed at 600 °C.

were incorporated into the $ZnAl_2O_4$ host lattice, coupled with the XRD results, further supporting the formation of a homogeneous $ZnAl_2O_4$:Mn solid solution (i.e. $Zn_{1-x}Mn_xAl_2O_4$) in the powder samples, which is responsible for the saturated green emissions under 458 nm excitation.

Fig. 7(a) shows the dependence of the PL spectra on various excitation wavelengths for samples annealed at 1200 °C. The PL spectra obtained at various excitation wavelengths only had a single emission peaking at 510 nm, and the emission intensities of the $ZnAl_2O_4$:Mn^{2+} phosphors were measured as a function of excitation wavelength. It seems that the Mn^{2+} ions can be excited by direct absorption into the 3d shell. Following excitation by the UV or visible light, the excited electrons relax to their lowest excited state ($^4T_1$), and then transition from $^4T_1$ to the ground state ($^6A_1$) of Mn^{2+}, emitting the green light. The green emission intensity clearly reached its highest value following a blue-light excitation at λ_{ex}=458 nm. The strongest excitation peak at 458 nm indicates that $ZnAl_2O_4$:Mn^{2+} is a potentially suitable green phosphor for white LEDs using blue LED chips. The dependence of the green emission intensity on the dopant concentration is plotted in Fig. 7(b). The emission intensity increased along with the dopant concentration, and reached a maximum at 3.0 mol% of Mn^{2+}. Subsequently the green emission decreased gradually because of concentration quenching. Therefore, the optimum doping concentration is determined to be approximately 3.0 mol%.

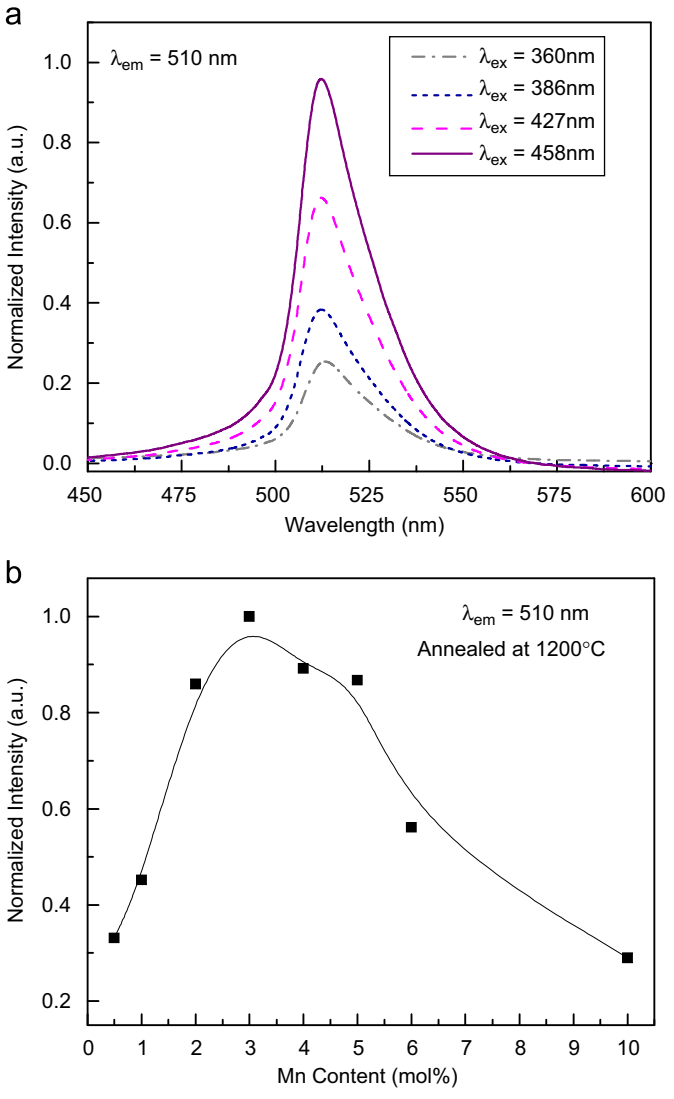

Fig. 7. Dependencies of the (a) PL spectra on various excitation wavelengths and (b) PL intensity on the Mn concentration under excitation at 458 nm; powder samples annealed at 1200 °C.

4. Conclusions

Mn-doped $ZnAl_2O_4$ nanocrystal phosphors have been prepared by a sol–gel process using zinc chloride, aluminum isopropoxide and manganese chloride as the precursors. Single-phase $ZnAl_2O_4$:Mn^{2+} powders possessing primary particle sizes less than ~50 nm were obtained with the processing temperature ≤ 1200 °C. Single-phase structure of zinc aluminate spinel began to crystallize at 600 °C. The FT-IR spectra indicated that the phosphors predominantly crystallized in a normal spinel structure. The PL spectra also confirmed the formation of homogeneous $Zn_{1-x}Mn_xAl_2O_4$ solid solutions. In addition to the crystallite size, the results also showed that the doping concentration had an effect on the homogeneity, degree of agglomeration and luminescence. Controlling the doping concentration and annealing temperature can thus significantly enhance the luminescence of $ZnAl_2O_4$:Mn^{2+} nanophosphors. The best PL emission of $ZnAl_2O_4$:Mn^{2+} is realized with excitation at 458 nm, indicating its good potential for use as a green phosphor for white LEDs using blue LED chips.

Acknowledgments

This work was supported by the National Science Council of Taiwan under Contract no. NSC 100–2221-E-150-044.

References

[1] J.H. Kim, P.H. Holloway, Enhancement of cathodoluminescence of $ZnGa_2O_4$:Mn thin-film phosphor by energetic particle bombardment, Applied Physics Letters 847 (2004) 2070–2072.
[2] L. Wang, X. Liu, Z. Hou, C. Li, P. Yang, Z. Cheng, H. Lian, J. Lin, Electrospinning synthesis and luminescence properties of one-dimensional Zn_2SiO_4:Mn^{2+} microfibers and microbelts, Journal of Physical Chemistry C 112 (2008) 18882–18888.
[3] S. Nakamura, G. Fasol, The Blue Laser Diode:GaN Based Light Emitters and Lasers, Springer, Berlin, 1997, p. 216.
[4] L. Chen, C.C. Lin, C.W. Yeh, R.S. Liu, Light converting inorganic phosphors for white light-emitting diodes, Materials 3 (2010) 2172–2195.
[5] R.J. Xie, N. Hirosaki, X.J. Liu, T. Takeda, H.L. Li, Crystal structure and photoluminescence of Mn^{2+}–Mg^{2+} codoped gamma aluminum oxynitride (γ-AlON): A promising green phosphor for white light emitting diodes, Applied Physics Letters 92 (2008) 201905.

[6] J. Wrzyszcz, M. Zawadzki, J. Trawczynski, H. Grabowska, W. Mista, Some catalytic properties of hydrothermally synthesised zinc aluminate spinel, Applied Catalysis A: General 210 (2001) 263–269.
[7] S. Farhadi, S. Panahandehjoo, Spinel-type zinc aluminate ($ZnAl_2O_4$) nanoparticles prepared by the co-precipitation method: a novel, green and recyclable heterogeneous catalyst for the acetylation of amines, alcohols and phenols under solvent-free conditions, Applied Catalysis A: General 382 (2010) 293–302.
[8] S.K. Sampath, J.F. Cordaro, Optical properties of zinc aluminate, zinc gallate, and zinc aluminogallate spinels, Journal of the American Ceramic Society 81 (1998) 649–654.
[9] Z. Lou, J. Hao, Cathodoluminescence of rare-earth-doped zinc aluminate films, Thin Solid Films 450 (2004) 334–340.
[10] H. Matsui, C.N. Xu, H. Tateyama, Stress-stimulated luminescence from $ZnAl_2O_4$:Mn, Applied Physics Letters 78 (2001) 1068–1070.
[11] G. Lakshminarayana, L. Wondraczek, Photoluminescence and energy transfer in Tb^{3+}/Mn^{2+} co-doped $ZnAl_2O_4$ glass ceramics, Journal of Solid State Chemistry 184 (2011) 1931–1938.
[12] C.J. Duan, W.M. Otten, A.C.A. Delsing, H.T. Hintzen, Preparation and photoluminescence properties of Mn^{2+}-activated $M_2Si_5N_8$ (M=Ca, Sr, Ba) phosphors, Journal of Solid State Chemistry 181 (2008) 751–757.
[13] J.G. Li, X.D. Li, X.D. Sun, T. Ishigaki, Monodispersed colloidal spheres for uniform Y_2O_3:Eu^{3+} red-phosphor particles and greatly enhanced luminescence by simultaneous Gd^{3+} doping, Journal of Physical Chemistry C 112 (2008) 11707–11716.
[14] C.C. Diao, C.F. Yang, Synthesis of high efficiency Zn_2SiO_4:Mn^{2+} green phosphors using nano-particles, Ceramics International 36 (2010) 1653–1657.
[15] M.T. Tsai, Y.X. Chen, P.J. Tsai, Y.K. Wang, Photoluminescence of manganese-doped $ZnAl_2O_4$ nanophosphors, Thin Solid Films 518 (2010) e9–e11.
[16] K.S. Sohn, B. Cho, H.D. Park, Photoluminescence behavior of manganese-doped zinc silicate phosphors, Journal of the American Ceramic Society 82 (1999) 2779–2784.
[17] J. Preudhomme, P. Tarte, Infrared studied of spinel-III: the normal II–III spinel, Spectrochimica Acta 27A (1971) 1817–1835.
[18] D. Mazza, M. Vallino, Mullite-type structures in the systems Al_2O_3–Me_2O (Me=Na, K) and Al_2O_3–B_2O_3, Journal of the American Ceramic Society 75 (1992) 1929–1934.
[19] P. McMillan, B. Piriou, The structures and vibrational spectra of crystals and glasses in the silica–alumina system, Journal of Non-Crystalline Solids 53 (1982) 279–298.
[20] W. Staszak, M. Zawadzki, J. Oka, Solvothermal synthesis and characterization of nanosized zinc aluminate spinel used in isobutane combustion, Journal of Alloys and Compounds 492 (2010) 500–507.
[21] A.A. da Silva, A.S. Goncalves, M.R. Davolos, Characterization of nanosized $ZnAl_2O_4$ spinel synthesized by the sol–gel method, Journal of Sol–Gel Science and Technology 49 (2009) 101–105.
[22] S. Mathur, M. Veith, M. Haas, H. Shen, N. Lecerf, V. Huch, S. Hufner, R. Haberkorn, H.P. Beck, M. Jilavi, Single-source sol–gel synthesis of nanocrystalline Zn Al_2O_4: structural and optical properties, Journal of the American Ceramic Society 84 (2001) 1921–1928.
[23] X. Duan, D. Yuan, X. Wang, H. Xu, Synthesis and characterization of nanocrystalline zinc aluminum spinel by a new sol–gel method, Journal of Sol–Gel Science and Technology 35 (2005) 221–224.
[24] V. Singh, R.P.S. Chakradhar, J.L. Rao, D.K. Kim, Characterization, EPR and luminescence studies of $ZnAl_2O_4$:Mn phosphors, Journal of Luminescence 128 (2008) 394–402.
[25] Y. Tanabe, S. Sugano, On the absorption spectra of complex ions, Journal of the Physical Society of Japan 9 (1954) 753–779.
[26] B.M. Tissue, Synthesis and luminescence of lanthanide ions in nanoscale insulating hosts, Chemistry of Materials 10 (1998) 2837–2845.
[27] M.T. Tsai, J.M. Wu, Y.F. Lu, H.C. Chang, Synthesis and luminescence characterization of manganese-activated willemite gel films, Thin Solid Films 520 (2011) 1027–1033.